CHEMISTRY OF MATERIALS

Article

pubs.acs.org/cm

Thermally, Operationally, and Environmentally Stable Organic Thin-Film Transistors Based on Bis[1]benzothieno[2,3-*d*:2′,3′-*d*′]naphtho[2,3-*b*:6,7-*b*′]dithiophene Derivatives: Effective Synthesis, Electronic Structures, and Structure–Property Relationship

Masahiro Abe,[†,‡] Takamichi Mori,[†] Itaru Osaka,[†] Kunihisa Sugimoto,[§] and Kazuo Takimiya*[,†]

[†]Emergent Molecular Function Research Group, RIKEN Center for Emergent Matter Science (CEMS), 2-1 Hirosawa, Wako, Saitama 351-0198, Japan

[‡]Center for Innovative Research (CIR), Research and Development Group, Nippon Kayaku Co., Ltd., 31-12 Shimo 3-Chome, Kita-ku, Tokyo 115-8588, Japan

[§]Japan Synchrotron Radiation Research Institute (JASRI), 1-1-1, Kouto, Sayo-cho, Sayo-gun, Hyogo 679-5198, Japan

Supporting Information

ABSTRACT: By developing an efficient synthetic route to the bis[1]benzothieno[2,3-*d*;2′,3′-*d*′]naphtho[2,3-*b*;6,7-*b*′]dithiophene (BBTNDT) framework, we have successfully synthesized new BBTNDT derivatives with phenyl (DPh-BBTNDT) or *n*-hexyl groups (C6-BBTNDT) at the 2 and 10 positions. Characterization of their vapor-deposited thin films revealed that, depending on the substituents introduced, their HOMO energy levels were slightly altered, and DPh-BBTNDT with the HOMO energy level of ca. 5.3 eV was supposed to be a stable organic semiconductor under ambient conditions. In fact, the DPh-BBTNDT-based OTFTs showed not only high mobility of up to 7.0 cm^2 V^{-1} s^{-1} under ambient conditions but also excellent operational and thermal stabilities up to 300 °C, whereas the parent and the hexyl derivative were less stable against the thermal treatments at high temperatures. The high mobility observed for the DPh-BBTNDT-based OTFTs can be correlated to the interactive packing structure in the bulk single crystal and thin film state of DPh-BBTNDT, which corroborates the existence of the well-balanced two-dimensional electronic structure in the solid state. With these excellent device characteristics, it can be concluded that DPh-BBTNDT is a promising and practical vapor-processable organic semiconductor, which can afford thermally, operationally, and environmentally stable OTFTs as well as high mobility.

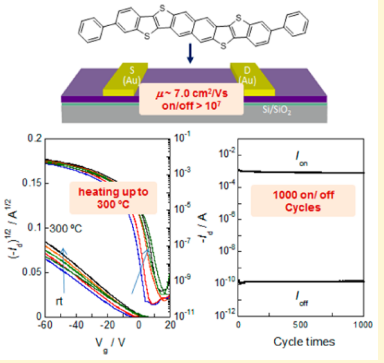

INTRODUCTION

Organic thin-film transistors (OTFTs) have attracted great interest for their potential use in electronic applications, including active-matrix displays, electronic paper, and chemical sensors.[1−3] In the last decades, the performances of OTFTs have been significantly improved,[4−7] and in particular, p-channel OTFTs have now realized many important achievements: high mobility (>3.0 cm^2 V^{-1} s^{-1}),[8−12] solution processability,[13,14] air-stability, flexibility, and low-voltage operation.[15] For these achievements, the development of new superior organic semiconductors have contributed significantly.

Among recently developed organic semiconductors, [1]-benzothieno[3,2-*b*][1]benzothiophene (BTBT) derivatives[6−18] and its π-extended homologues, such as dinaphtho[2,3-*b*;2′,3′-*f*]thieno[3,2-*b*]thiophene (DNTT),[19−22] have been focused as promising organic semiconductors capable of affording OTFTs with high mobility and environmental stability (Figure 1),[23] which can be further utilized in various sophisticated device applications.[24−26] In order to improve the performances of

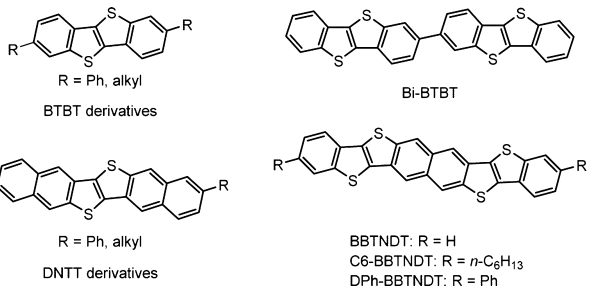

Figure 1. Molecular structures of BTBTs and related compounds.

OTFTs, extension of π-conjugation system of organic semiconductors has been one of the most effective ways, as well exemplified by the acene-based organic semiconductors.[27,28]

Received: April 30, 2015
Revised: June 7, 2015
Published: June 9, 2015

DOI: 10.1021/acs.chemmater.5b01608
Chem. Mater. 2015, 27, 5049−5057

This is also the case for BTBT and related materials, and thus, largely π-extended systems based on the BTBT framework has recently been examined;[29−31] for example, Yu and co-workers have reported a BTBT covalently linked dimer, 2,2′-bi[1]-benzothieno[3,2-*b*][1]benzothiophene (Bi-BTBT, Figure 1), which affords vapor processed TFTs showing mobility as high as 2.1 $cm^2 V^{-1} s^{-1}$ with excellent thermal stability up to 250 °C. Much higher mobility up to 5.6 $cm^2 V^{-1} s^{-1}$ has been reported for a BTBT-fused dimer, bis[1]benzothieno[2,3-*d*;2′,3′-*d*′]-naphtho[2,3-*b*;6,7-*b*′]dithiophene (BBTNDT).[32] It should be noted that the mobility reported for the BBTNDT-based OTFTs are among the highest for OTFTs based on thienoacenes without substituents. On the other hand, introduction of substituents, such as long alkyl groups and aromatic rings has been another promising molecular modification to develop high-performance organic semiconductors. This has been well exemplified by the superior OTFTs with enhanced mobilities based on BTBT and DNTT derivatives with alkyl or phenyl groups along the molecular long axis direction. In particular, introduction of long alkyl groups on BTBT or DNTT tends to help intermolecular interaction in the condensed phase via intermolecular van deer Waals interaction of the alkyl groups, which is believed to enhance mobilities of their devices.[17,18,33] On the other hand, the introduced phenyl groups on DNTT can enhance thermal stability of not just the compounds themselves but also the thin films used in the OTFT devices, affording thermally stable OTFTs.[34,35] With these preceding results in mind, we have designed new BBTNDT derivatives with alkyl or phenyl substituents at the 2,10-positions, which correspond to the molecular long axis direction (Figure 1). We report here a new efficient synthesis of BBTNDT derivatives, their electronic structures, single crystal and thin film structures, and OTFT performances. OTFT devices based on new BBTNDT derivatives demonstrated high mobility of up to 7.0 $cm^2 V^{-1} s^{-1}$ with excellent thermal, environmental, and operational stability.

RESULTS AND DISCUSSIONS

Synthetic Strategy and Actual Synthesis. The synthesis of parent BBTNDT previously reported includes a thiophene ring formation reaction via the Pd-catalyzed intramolecular aryl−aryl coupling[32] of the phenylthio groups at 3- and 8-positions on naphtho[2,3-*b*:6,7-*b*′]dithiophene derivatives (**1**, R = H) (Route 1 in Scheme 1). For the syntheses of 2,10-disubstituted BBTNDT derivatives, however, this strategy can potentially afford isomers because the precursor has two structurally distinct reaction sites on each phenyl ring. To avoid such undesired reaction, we have employed a thiophene annulation reaction via the acid-mediated aryl-sulfide bond formation reaction[36−38] from naphthalene derivatives with two benzo[*b*]thiophene- and methylsulfinyl- substituents (**2**) (Route 2 in Scheme 1), which are supposed to selectively afford 2,10-disubstituted BBTNDT derivatives.

According to the second route depicted in Scheme 1, we first carried out the synthesis of parent BBTNDT (Scheme 2). The

Scheme 1. Synthetic Strategy of 2,10-Disubstituted BBTNDT Derivatives[a]

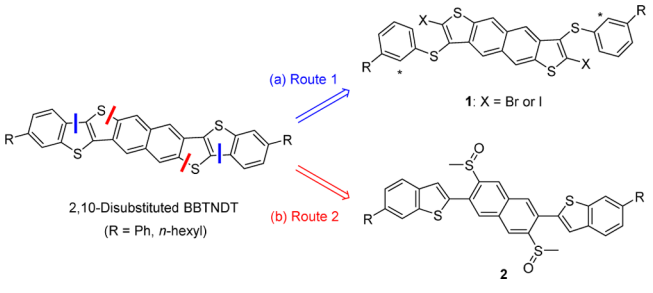

[a](a) Previously reported route via the intramolecular aryl−aryl coupling reaction. Note that two possible reaction sites on the phenyl moieties including undesirable positions marked with asterisk affording isomeric byproducts. (b) Newly proposed route via the acid-mediated aryl-sulfide bond formation reaction.

Scheme 2. Syntheses of BBTNDT Derivatives

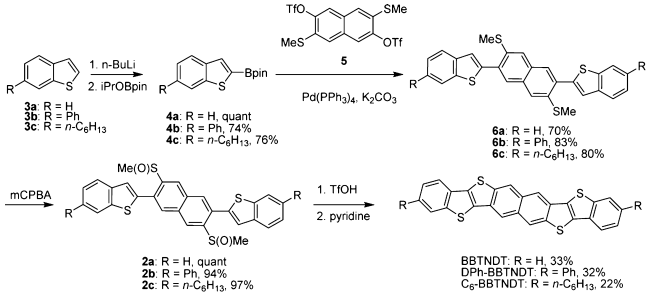

Suzuki−Miyaura coupling reaction between 2-(4,4,5,5-tetramethyl-1,3,2-dioxaborolan-2-yl)benzo[*b*]thiophene (**4a**)[39] and 2,6-bis(methylthio)-3,7-bis(trifluoromethanesulfonyloxy)-naphthalene (**5**)[32] afforded 2,6-bis(benzo[*b*]thiophen-2-yl)-3,7-bis(methylthio)naphthalene (**6a**), which was quantitatively converted into the precursor, 2,6-bis(benzo[*b*]thiophen-2-yl)-3,7-bis(methylsulfinyl)naphthalene (**2a**). The final cyclization reaction and following purification by repeated vacuum sublimation afford parent BBTNDT in a moderate yield (33%). The total yield of BBTNDT from **5** by the present approach was ca. 23% in three steps, which is better than the previous approach (Route 1 with R = H in Scheme 1), where the total yield of BBTNDT from **5** was 20−27% (four steps) before purification.

For the syntheses of the BBTNDT derivatives, we employed readily available 6-bromobenzo[*b*]thiophene,[40] which can be effectively converted into 6-phenyl- (**3b**) and 6-hexylbenzo[*b*]-thiophene (**3c**). Borylation at the 2-position of **3b** and **3c** gave **4b** and **4c**, respectively, which were utilized in the Suzuki−Miyaura coupling reaction with **5** to give corresponding 2,6-bis(benzo[*b*]thiophen-2-yl)-3,7-bis(methylthio)naphthalenes (**6b** and **6c**) in good yields. Oxidation of the methylthio groups on **6** proceeded smoothly to give the precursors (**2b** and **2c**), and the thiophene annulation reaction followed by sublimation afforded the corresponding BBTNDT derivatives in moderate yields.

Electronic Properties. In order to evaluate the HOMO energy levels of the BBTNDT derivatives, ionization potentials (IPs) of their vacuum-deposited thin films on ITO substrates were measured with photoemission yield spectroscopy in air (Figure 2a). The IPs of BBTNDT, DPh-BBTNDT, and C6-BBTNDT are 5.1, 5.3, and 5.0 eV, respectively, which are just above or around of 5.0 eV, a borderline of air stability for p-channel organic semiconductors.[41−45] It should be noted that the introduction of hexyl groups affords the slightly smaller IP than the parent, whereas the phenyl derivative has the larger IP, indicating that the latter is likely a stable organic semiconductor (vide infra).

DOI: 10.1021/acs.chemmater.5b01608
Chem. Mater. 2015, 27, 5049−5057

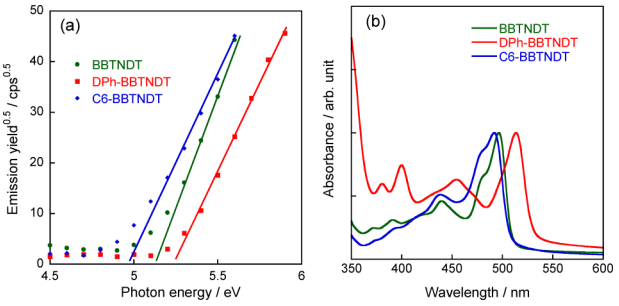

Figure 2. Photoemission yield spectroscopy in air (a) and UV–vis absorption spectra (b) of BBTNDT, DPh-BBTNDT, and C6-BBTNDT measured on evaporated thin films.

UV–vis absorption spectra of the thin films on quartz substrates are shown in Figure 2b. For the DPh-BBTNDT thin film, the absorption peak at around 513 nm corresponds to the π–π^* transition shifted bathochromicaly by ca. 20 nm than that of the BBTNDT thin film, which can be ascribed to additional π-conjugation. On the other hand, C6-BBTNDT showed no clear shift from the parent one. This is contrasted to the tendency observed in the substituted DNTT derivatives (Supporting Information Figure S1), where introduction of the phenyl or alkyl groups on the molecular long axis direction causes clear bathochromic shifts.[33,34] Although the reasons for the different effects caused by the alkyl substitution in the two systems are not clear, the more π-extended BBTNDT core than DNTT could be less sensitive in the electronic structure by derivatization. These optical properties of three compounds are summarized in Table 1 together with their HOMO energy levels estimated from the IP values.

Table 1. Electronic Properties of BBTNDT Derivatives

compound	E_{HOMO}/eV[a]	λ_{max}/nm[b]	λ_{edge}/nm[b]	E_g/eV[c]
BBTNDT	−5.1	494	515	2.4
DPh-BBTNDT	−5.3	513	535	2.3
C6-BBTNDT	−5.0	492	505	2.5

[a]Determined by photoemission yield spectroscopy in air. E_{HOMO} was defined as −(IP) in eV. [b]From absorption spectra measured on evaporated thin films. [c]Calculated from λ_{edge}.

OTFT Devices with Vapor-Deposited Thin Film. OTFT devices of the new BBTNDT derivatives were fabricated on alkyltrichlorosilane-treated Si/SiO_2 substrates with a bottom gate–top contact device configuration using their vapor-deposited films and were evaluated under ambient conditions. Table 2 summarizes the OTFT characteristics of the devices fabricated on the octadecyltrichlorosilane (ODTS)-treated Si/SiO_2 substrate at different substrate temperatures during thin-film deposition (T_{sub}). As depicted in Figure 3, the devices fabricated on the ODTS-treated substrates (T_{sub} = 200 °C) showed text-book like transfer and output characteristics with relatively high hole mobilities. The DPh-BBTNDT-based devices gave higher mobilities than those of C6-BBTNDT- or BBTNDT-based devices. It is interesting to note that both derivatives tend to afford better performances in the devices fabricated at the higher substrate temperatures (T_{sub}s), and the maximum mobilities were recorded for T_{sub}s = 200 °C for both compounds. In particular, the best mobility of up to 7.0 cm^2 V^{-1} s^{-1} was observed for the DPh-BBTNDT-based devices, which is higher than that of the mobility of the parent

Table 2. Transistor Characteristics of DPh-BBTNDT and C6-BBTNDT Fabricated on ODTS-Treated Si/SiO_2[a] Substrate

compound	T_{sub}/°C	μ_{FET}/cm^2 $V^{-1}s^{-1}$ [b]	I_{on}/I_{off}	V_{th}/V[c]
DPh-BBTNDT	rt	0.98 (0.65)	10^5	−11.2
	100	3.9 (3.6)	10^6	−2.5
	150	4.5 (4.1)	10^6	−3.2
	200	7.0 (6.3)	10^7	−5.2
C6-BBTNDT	rt	0.26 (0.20)	10^5	2.8
	100	0.41 (0.25)	10^6	1.1
	150	1.0 (0.54)	10^6	0.1
	200	1.8 (1.2)	10^6	3.3
BBTNDT[d]	100	5.6 (4.7)	10^7	−6.0

[a]See Supporting Information Table S1 for device characteristics on the OTS and HMDS treated substrate. [b]Extracted from the saturated regime (V_d = V_g = −60 V). The values in parentheses are averaged ones from more than ten devices [c]Average value. [d]See ref 32.

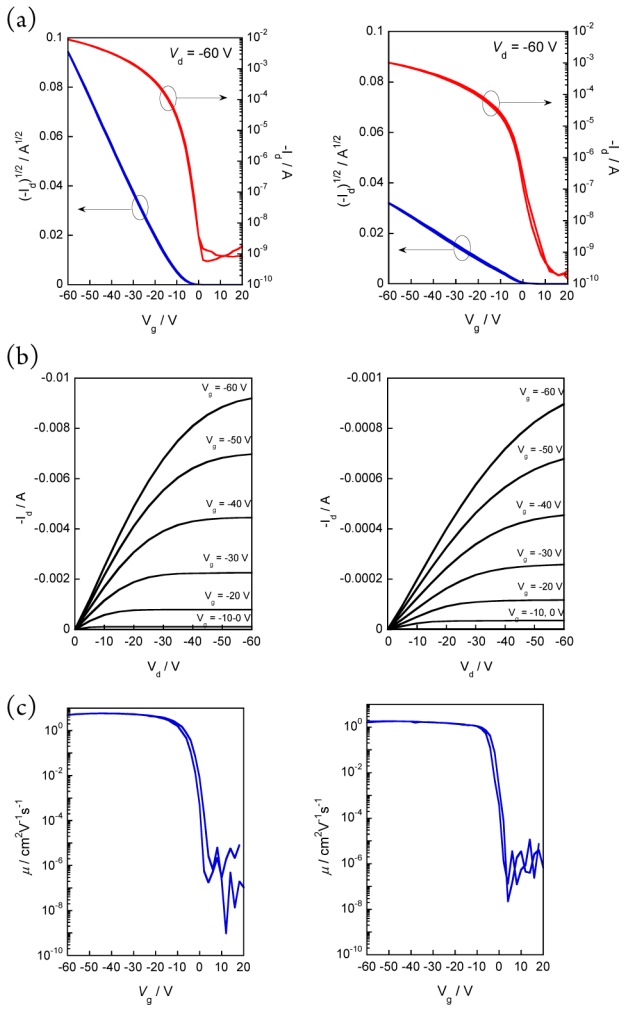

Figure 3. Transfer (a), output (b), and gate-voltage (V_g) dependence of mobility (c) of DPh-BBTNDT (left) and C6-BBTNDT (right).

BBTNDT-based devices (5.6 cm^2 V^{-1} s^{-1})[32] and comparable with the highest mobility so far reported for small-molecule-based OFETs with polycrystalline thin films as the active semiconducting channel.[44–46] We also investigated gate-voltage (V_g) dependence of the mobility (Figure 3c). In both the derivatives, the mobility sharply rose up at the subthreshold

DOI: 10.1021/acs.chemmater.5b01608
Chem. Mater. 2015, 27, 5049–5057

regime and kept constant up to high gate voltage, indicating that the mobility is independent of V_g. This suggests that there is no overestimation of the mobilities.

Single Crystal X-ray Analysis of DPh-BBTNDT. It is important to correlate the transport properties of the devices and the packing structures of semiconducting molecules in the condensed phase, which can rationalize the device performances from the structural point of view. Single crystals of DPh-BBTNDT with suitable quality for single crystal X-ray analysis were obtained by physical vapor transport,[47] though all attempts to prepare single crystals of C6-BBTNDT were failed. Depicted in Figure 4 are the molecular and packing structures

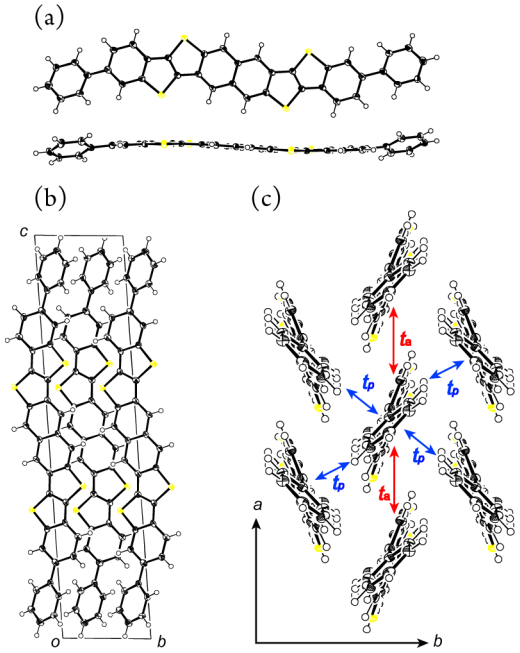

Figure 4. Structure of DPh-BBTNDT: (a) molecular structure, (b) packing structure projected along the crystallographic *a*-axis, and (c) herringbone packing structure in the crystallographic *ab* cell. Calculated intermolecular transfer integrals of HOMOs are t_a = 71 and t_p = 43 meV.[48]

of DPh-BBTNDT. The molecule has an almost planar BBTNDT core with the maximum deviation of 0.14 Å from the mean plane and two phenyl groups with dihedral angles of ca. 26.6° (Figure 4a). In the packing structure, the molecules form a layered structure along the crystallographic *c*-axis direction (Figure 4b), and in each layer, the molecular arrangement is classified into the herringbone packing (Figure 4c) similar to that of parent BBTNDT[32] and related BTBT and DNTT derivatives.[23] Calculated intermolecular transfer integrals of HOMOs in the herringbone cell are 71 meV for the stacking pairs along the *a*-axis (1 0 0) direction (t_a) and 43 meV for the side-by-side pairs along the (1 1 0) and (−1 1 0) directions (t_p) (Figure 4c).[48] Although these values are almost comparable with those calculated for the BBTNDT single crystal, 75 meV for the stacking pairs and 32 and 41 meV for the side-by-side pairs, the values for the two directions are much balanced in DPh-BBTNDT, indicating that the electronic structure of DPh-BBTNDT is more two-dimensional (2D)-like and isotropic (Supporting Information Figure S2). The enhanced mobility observed for the DPh-BBTNDT-based devices compared with the parent BBTNDT devices thus can be rationalized by better isotropic electronic structure.[49]

Evaluation of Vapor Deposited Thin Films. The above discussion on the electronic structure based on the single crystal analysis is consistent with the empirical high mobility of the DPh-BBTNDT-based devices. On the other hand, the device characteristics were evaluated with the vapor-deposited thin films, and thus, we further characterized the thin films by means of atomic force microscopy (AFM) and thin film X-ray diffraction (XRD). Figure 5 shows the AFM images of the thin

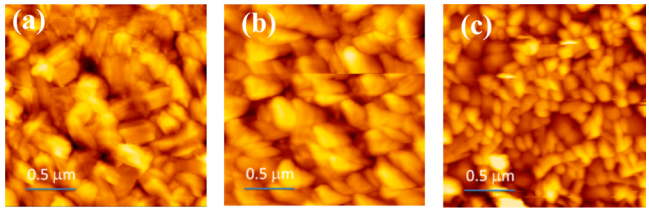

Figure 5. AFM images (2 × 2 μm) of evaporated thin films on the Si/SiO_2 substrate affording the best device characteristics: (a) DPh-BBTNDT, (b) C6-BBTNDT, and (c) BBTNDT on the ODTS-treated substrate (T_{sub} = 200 °C for DPh- and C6-BBTNDT and T_{sub} = 100 °C for BBTNDT).

films of DPh-BBTNDT and C6-BBTNDT evaporated at T_{sub} = 200 °C on the ODTS-treated Si/SiO_2 substrate, together with that of parent BBTNDT (T_{sub} = 100 °C). All three compounds gave similar surface morphologies with crystalline grains of similar sizes. The grain sizes of these compounds depend on T_{sub} as observed for many related organic semiconducting materials (Supporting Information Figure S3), and apparently, the larger grains at higher T_{sub}s contribute to the higher mobility both for DPh-BBTNDT and C6-BBTNDT.

Figure 6 shows the out-of-plane and in-plane XRDs of DPh- and C6-BBTNDT thin films deposited on the Si/SiO_2 substrate, and the structural parameters both obtained from the thin film XRDs and single crystal analysis are summarized in Table 3 together with those of the parent BBTNDT.[32] Obviously, from the out-of-plane XRDs, both molecules have an edge-on orientation to the substrate surface, similar to the parent BBTNDT thin film (Supporting Information Figure S4). The interlayer spacing (*d*-spacing) of DPh-BBTNDT (28.9 Å) is similar to or slightly longer than the molecular length obtained from the single crystal X-ray analysis (27.6 Å) and the optimized molecular structure by the DFT calculations (28.1 Å), corresponding to a model where the molecules stand perpendicular to the substrate surface. In contrast, the *d*-spacing of C6-BBTNDT, 32.5 Å, is shorter than one obtained from the optimized molecular geometry (33.4 Å, see also Supporting Information Figure S5), implying that C6-BBTNDT molecules tilt to the substrate normal or the alkyl layers slightly interdigitate, which anyway might cause less effective intermolecular orbital coupling, in turn resulting in relatively low mobility.

In the in-plane XRDs of the DPh-BBTNDT thin film, three characteristic peaks assignable to the herringbone *ab* cell (110, 020, and 120 reflections) were clearly observed and calculated length of the *a* and *b* crystallographic axis from these three peaks are well matched with those in the single crystal data (Table 3). Similarly three peaks were also observed in the in-plane XRD of the C6-BBTNDT thin film (Figure 6b, right). Although the single crystal data of C6-BBTNDT could not be

DOI: 10.1021/acs.chemmater.5b01608
Chem. Mater. 2015, 27, 5049−5057

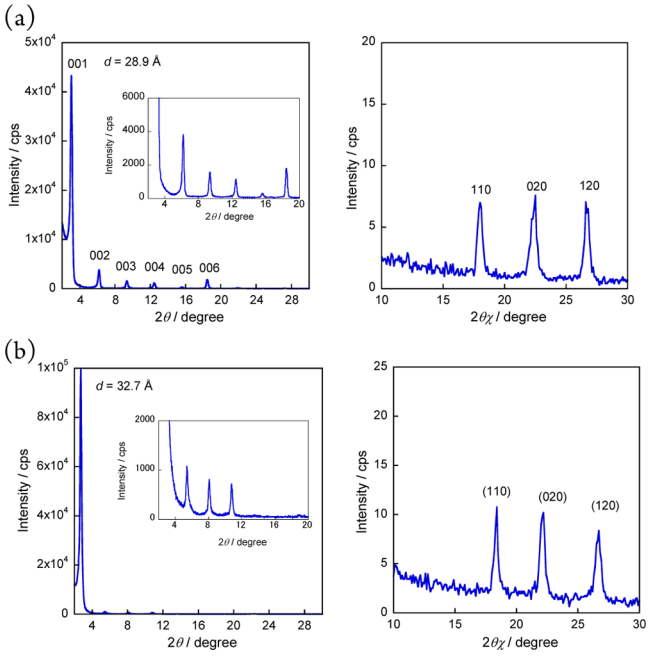

Figure 6. Out-of-plane (left) and in-plane (right) XRD patterns of evaporated film on the Si/SiO_2 substrate: (a) DPh-BBTNDT and (b) C6-BBTNDT on the ODTS-treated substrate. The indexes in panel a are based on the bulk single crystal cell, whereas the indexes in the parentheses in panel b are assigned based on the similarity to that of DPh-BBTNDT.

available, the length of *a* and *b* axes are estimated from three peaks in the in-plane XRD, provided that the unit cell is of monoclinic or higher symmetry, that is, at least, $\alpha = \gamma = 90°$, similar to those of BBTNDT and DPh-BBTNDT. The estimated *a*-axis length of C6-BBTNDT is ca. 6.0 Å, which is similar to those of DPh-BBTNDT and parent BBTNDT. On the other hand, the *b*-axis length, ca. 8.0 Å is apparently longer than those of DPh-BBTNDT (ca. 7.6 Å) and the parent (ca. 7.8 Å). The crystallographic *b* axis can be related to the edge-to-face intermolecular interaction (see Figure 4c), and the longer *b* axis of C6-BBTNDT than those of others strongly imply its less effective intermolecular orbital coupling in this directions. Although the quantitative evaluation of the transfer integrals of C6-BBTNDT was not possible, the present structural characterization can qualitatively afford the reasons for relatively lower mobility of C6-BBTNDT-based devices than those of other BBDNDT derivatives.

Stability of OTFT Devices. In the recent advanced applications of OFETs, stabilities of devices against various factors, such as thermal treatment, repeated operations, and environmental conditions, are regarded as important issues,[25,34,35] and thus, we carried out various stability tests of the BBTNDTs-based devices. We first examine continuous operation of the devices by alternately applying V_g of 0 and −30 V at V_d = −30 V for 1000 cycles. As shown in Figure 7,

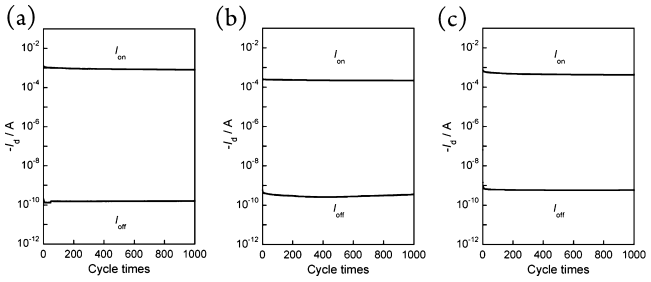

Figure 7. Operational stability test of (a) DPh-BBTNDT-, (b) C6-BBTNDT-, and (c) BBTNDT-based devices by alternately applying V_G of 0 and −30 V at V_{DS} = −30 V for 1000 cycles.

excellent operational stability of the devices, as confirmed by the nearly negligible change of both on and off current, was observed for all the devices based on three BBTNDT derivatives.

To evaluate the thermal stability of the BBTNDTs-based OTFTs, the device characteristics were measured after thermal treatments for 30 min at gradually raised temperatures from 100 to 300 °C. As demonstrated in Figure 8, the devices with different BBTNDT derivatives as the active semiconducting layer showed distinct behaviors upon thermal treatments. Among them, the most noticeable degradation was observed for the C6-BBTNDT-based device, where a clear off-current increase upon thermal treatment took place (Figure 8b). This can be explained by its relatively smaller IP (5.0 eV) than those of other BBTNDT derivatives; the thermal treatment may accelerate oxidation of the semiconducting material by the ambient oxygen. The parent BBTNDT-based devices also showed gradual off-current increase and relatively large threshold voltage (V_{th}) shift (ca. 15 V with the thermal treatment at 300 °C, Figure 8c). On the other hand, the DPh-BBTNDT-based devices was not very sensitive to the thermal treatment; although a small V_{th} shift of ca. 5 V was observed, the off current was still low even after the treatment at 300 °C, keeping large on/off ratio over 10^7, which clearly demonstrates its outstanding thermal stability (Figure 8a). The excellent thermal stability of DPh-BBTNDT-based devices can be rationalized by considering its relatively large IP (5.3 eV) and tight packing structure assisted by the phenyl groups, which intermolecularly interact with the phenyl moieties of adjacent molecules via the CH−π hydrogen bond-like interactions (Figure 4b and c).

Table 3. Structural Parameters of *ab* Cell Extracted from XRDs

compound	*d*-spacing[a]/Å	molecular length (*l*)/Å[b]	*a*(*c*)/Å[c]	*b*/Å[d]
DPh-BBTNDT	28.9	27.6 (28.1)	6.1280(5) (6.1)	7.581(2) (7.6)
C6-BBTNDT	32.5	−(33.4)	−(6.0)	−(8.0)
BBTNDT[e]	20.3	19.3 (19.6)[d]	5.9894(3) (5.9)	7.807(1) (7.8)

[a]Calculated interlayer spacing from the 001 reflection for DPh- and C6-BBTNDTs and the 100 reflection for BBTNDT. [b]Obtained from single crystal X-ray analysis. Values in parentheses are obtained from molecular geometry optimized by the DFT calculations (B3LYP/6-31G*). [c]Length of the crystallographic axis in the stacking direction. The crystallographic *a* axis corresponds to the DPh-BBTNDT single crystal, whereas the *c* axis to the parent BBTNDT. The values in parentheses are estimated from the in-plane XRD data. [d]Length of crystallographic *b* axis (the side-by-side direction). The values in parentheses are estimated from the in-plane XRD data. [e]See ref 32.

DOI: 10.1021/acs.chemmater.5b01608
Chem. Mater. 2015, 27, 5049−5057

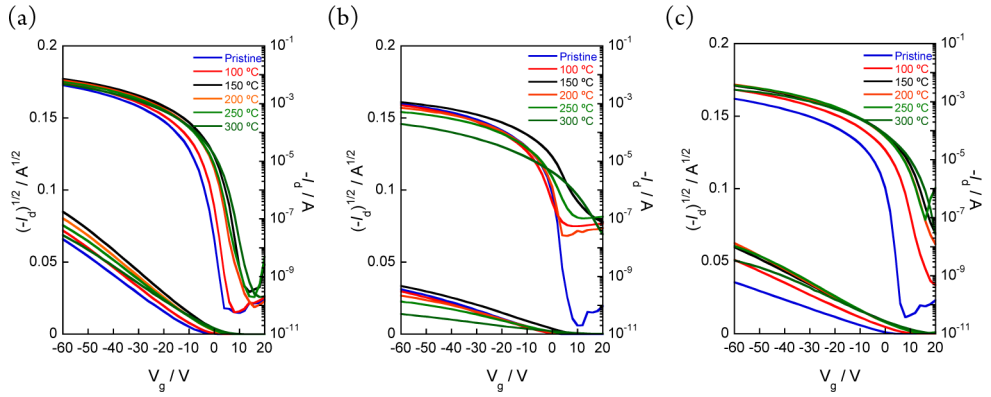

Figure 8. Transfer curves of (a) DPh-BBTNDT-, (b) C6-BBTNDT-, and (c) BBTNDT-based OFET devices upon annealing up to 300 °C measured under ambient conditions at $V_d = -60$ V.

CONCLUSION

In the present work, we have developed an effective and general synthetic route to BBTNDT derivatives. With the new synthetic route, two BBTNDT derivatives, DPh-BBTNDT and C6-BBTNDT, were synthesized. Evaluation of their electronic properties by using their vapor-deposited thin films demonstrated that DPh-BBTNDT with two phenyl groups in the molecular long axis direction has relatively large IP than that of the parent, whereas C6-BBTNDT smaller IP. By evaluating further the BBTNDT derivatives including the parent one using the OTFT configuration, DPh-BBTNDT was turned out to be the most superior one affording vapor-processed OTFT devices showing very high hole mobility (~7.0 cm^2 V^{-1} s^{-1}) with excellent operational and thermal stabilities (up to 300 °C). The high mobility of the devices can be explained by its isotropic two-dimensional (2D) electronic structure elucidated by XRDs and theoretical calculations. The good thermal stability can be assisted by its relatively large IP (5.3 eV) and the tight and interactive packing structure in the thin film state. Thus, we believe that DPh-BBTNDT is a promising and practical vapor-processable organic semiconductor, which can afford thermally, operationally, and environmentally stable OTFTs showing very high mobility, and will be utilized into sophisticated device applications in the future.

EXPERIMENTAL SECTION

General. All chemicals and solvents are of reagent grade unless otherwise indicated. Tetrahydrofuran (THF), *N*,*N*-dimethylformamide (DMF), dichloromethane, and toluene were purified with standard distillation procedures prior to use. 3,7-Bis(methylthio)-2,6-bis-(trifluoromethanesulfonyloxy)naphthalene (**5**),[32] 2-(4,4,5,5-tetramethyl-1,3,2-dioxaborolan-2-yl)benzo[*b*]thiophene (**4a**),[39] and 6-bromobenzo[*b*]thiophene[40] were prepared according to the literatures. All reactions were carried out under nitrogen atmosphere. Melting points were uncorrected. NMR spectra were obtained in deuterated chloroform ($CDCl_3$) with TMS as the internal reference; chemical shifts (δ) are reported in parts per million, unless otherwise stated. EI-MS spectra were obtained using an electron impact ionization procedure (70 eV).

*6-Phenylbenzo[b]thiophene (**3b**).* A solution of 6-bromobenzo-[*b*]thiophene (8.56 g, 40.0 mmol), phenylboronic acid (5.85 g, 48.0 mmol), and potassium carbonate (11.06 g, 80.0 mmol) in DMF (600 mL) and water (30 mL) was deaerated by argon stream for 30 min. To the solution was added $Pd(PPh_3)_4$ (2.31 g, 2.0 mmol), and the mixture was heated at 90 °C for 12h, cooled to rt, and poured into water (600 mL). The organic layer was separated and the aqueous layer was extracted with ethyl acetate (300 mL × 2). The combined organic layers were washed with brine (200 mL), dried ($MgSO_4$), and evaporated in vacuo. The residue was purified by column chromatography on silica gel eluted with hexane to afford **3b** (6.95 g, 83%) as a white solid. Mp 51.5 °C. ^{1}H NMR (400 MHz) δ 7.32−7.38 (m, 1H), 7.34 (d, J = 5.2 Hz, 1H), 7.41−7.49 (m, 2H), 7.44 (d, J = 5.2 Hz, 1H), 7.60 (dd, J = 1.6, 8.4 Hz, 1H), 7.63−7.67 (m, 2H), 7.86 (d, J = 8.4 Hz, 1H), 8.08 (s, 1H). ^{13}C NMR (100 MHz) δ 120.9, 123.7, 123.9, 124.1, 126.8, 127.3, 127.5, 128.9, 137.7, 138.8, 140.6, 141.2. MS (EI) m/z = 210 (M^+). Anal. calcd for $C_{14}H_{10}S$: C, 79.96; H, 4.79%. Found C, 79.95; H, 4.89%.

*6-Hexylbenzo[b]thiophene (**3c**).* A solution of 9-BBN (0.5 M solution in THF, 98 mL, 49 mmol) and 1-hexene (4.12 g, 49 mmol) were stirred for 15 h at room temperature. To the mixture was added $PdCl_2$(dppf) (41 mg, 0.05 mmol), 6-bromobenzo[*b*]thiophene (7.49 g, 35 mmoI) in deaerated solution of sodium hydroxide (1.96 g, 49 mmol) in water (20 mL) at rt, and the resulting mixture was refluxed for 24 h. After cooling, the mixture was diluted with water (100 mL) and extracted with chloroform (100 mL × 2). The combined extracts were dried ($MgSO_4$), concentrated in vacuo, and purified by column chromatography on silica gel eluted with hexane to give **3c** (7.11 g, 93%) as colorless oil. ^{1}H NMR (400 MHz) δ 0.88(t, J = 7.2 Hz, 3H), 1.25−1.40 (m, 6H), 1.62−1.71 (m, 2H), 2.72 (t, J = 7.8 Hz, 2H), 7.19 (dd, J = 1.2, 8.0 Hz, 1H), 7.28 (dd, J = 0.8, 5.6 Hz, 1H), 7.35 (d, J = 5.6 Hz, 1H), 7.68 (d, J = 1.2 Hz, 1H), 7.72 (d, J = 8.4 Hz, 1H). ^{13}C NMR (100 MHz) δ 14.3, 22.8, 29.1, 31.8, 31.9, 36.2, 121.8, 123.3, 123.7, 125.3, 125.5, 137.7, 139.3, 140.1. MS (EI) m/z = 232 (M^+). Anal. Calcd for $C_{14}H_{18}S$: C, 77.01; H, 8.31%. Found C, 77.08; H, 8.30%.

*6-Phenyl-2-(4,4,5,5-tetramethyl-1,3,2-dioxaborolan-2-yl)benzo-[b]thiophene (**4b**).* To a solution of **3b** (3.15 g, 15.0 mmol) in THF (30 mL) was added 1.6 M hexane solution of *n*-BuLi (13.1 mL, 21.0 mmol) at −78 °C. After the mixture was stirred for 1 h at rt, 2-isopropyloxy-4,4,5,5-tetramethyl-1,3,2-dioxaborolane (4.18 g, 22.5 mmol) was added to the solution at −78 °C, and the resulting mixture was stirred for 19 h at rt. The mixture was poured into water (100 mL) and was extracted with ethyl acetate (100 mL × 2). The combined extracts were washed with water (100 mL) and brine (100 mL × 2), dried ($MgSO_4$), and concentrated in vacuo. The residue was purified by column chromatography on silica gel eluted with chloroform to give **4b** (3.75 g, 74%) as yellow oil. ^{1}H NMR (400 MHz) δ 1.39 (s, 12H), 7.33−7.39 (m, 1H), 7.43−7.49 (m, 2H), 7.60 (dd, J = 1.2, 8.4 Hz, 1H), 7.66−7.69 (m, 2H), 7.90 (d, J = 8.4 Hz, 1H), 7.90 (s, 1H), 8.11 (d, J = 0.8 Hz, 1H). ^{13}C NMR (100 MHz) δ 24.9, 84.6, 120.9, 124.1, 124.6, 127.5(× 2), 128.9, 134.2, 138.7, 139.7, 141.1, 144.6. MS (EI) m/z = 358 (M^+). Anal. calcd for $C_{20}H_{21}BO_2S$: C, 71.44; H, 6.30%. Found C, 71.14; H, 6.34%.

*6-Hexyl-2-(4,4,5,5-tetramethyl-1,3,2-dioxaborolan-2-yl)benzo[b]-thiophene (**4c**).* To a solution of **3c** (1.26 g, 5.8 mmol) in THF (15 mL) was added 1.6 M hexane solution of *n*-BuLi (5.0 mL, 8.0 mmol) at −78 °C. After the mixture was stirred for 1 h at rt, 2-isopropoxy-4,4,5,5-tetramethyl-1,3,2-dioxaborolane (1.61 g, 8.7 mmol) was added to the solution at −78 °C, and the resulting mixture was stirred for 19

DOI: 10.1021/acs.chemmater.5b01608
Chem. Mater. 2015, 27, 5049−5057

h at rt. The mixture was poured into water (100 mL) and was extracted with ethyl acetate (100 mL × 2). The combined extracts were washed with water (100 mL) and brine (100 mL × 2), dried ($MgSO_4$), and concentrated in vacuo. The residue was purified by column chromatography on silica gel eluted with chloroform to give **4c** (1.83 g, 92%) as yellow oil. ^{1}H NMR (400 MHz): δ 0.88 (t, J = 7.2 Hz, 3H), 1.25−1.36 (m, 6H), 1.36 (s, 12H), 1.61−1.70 (m, 2H), 2.71 (t, J = 8.0 Hz, 2H), 7.17 (dd, J = 1.6, 8.4 Hz, 1H), 7.69 (s, 1H), 7.74 (d, J = 8.4 Hz, 1H), 7.83 (s, 1H). ^{13}C NMR (100 MHz) δ 14.2, 22.7, 24.9, 29.1, 31.7, 31.8, 36.2, 84.4, 121.7, 124.1, 125.6, 134.5, 138.6, 140.7, 144.2. MS (EI) m/z = 344 (M^+). Anal. calcd for $C_{20}H_{29}BO_2S$: C, 69.77; H, 8.49%. Found C, 69.63; H, 8.57%.

*2,6-Bis(benzo[b]thiophen-2-yl)-3,7-bis(methylthio)naphthalene (**6a**).* To a degassed solution of 2-(4,4,5,5-tetramethyl-1,3,2-dioxaborolan-2-yl)benzo[*b*]thiophene (**4a**, 5.00 g, 19.2 mmol), 3,7-bis(methylthio)-2,6-bis(trifluoromethanesulfonyloxy)naphthalene (**5**, 4.13g, 8.00 mmol), and K_2CO_3 (4.42 g, 32.0 mmol) in DMF (100 mL) and water (5.0 mL) was added $Pd(PPh_3)_4$ (0.924 g, 0.800 mmol). The mixture was then heated at 90 °C for 12 h, cooled to rt, poured into hydrochloric acid (1 M, 200 mL), filtered, and washed with water and methanol to give **6a** (2.73 g, 70%) as a yellow solid. Mp 295.9 °C. ^{1}H NMR (400 MHz) δ 2.54 (s, 6H), 7.35−7.43 (m, 4H), 7.59 (s, 2H), 7.50 (s, 2H), 7.83−7.91 (m, 4H), 7.88 (s, 2H). ^{13}C NMR (100 MHz) δ 16.2, 122.2, 123.0, 124.0, 124.5, 124.6, 124.8, 129.0, 130.9, 132.7, 136.3, 140.0, 140.4, 140.9. MS (EI) m/z = 484 (M^+). HRMS (APCI) m/z calcd for $C_{28}H_{21}S_4$ $[MH]^+$: 485.0526. Found: 485.0533.

*2,6-Bis(6-phenylbenzo[b]thiophen-2-yl)-3,7-bis(methylthio)-naphthalene (**6b**).* To a degassed solution of **4b** (2.42g, 7.2 mmol), **5** (1.55 g, 3.0 mmol), and K_2CO_3 (1.66 g, 12.0 mmol) in DMF (70 mL) and water (3.5 mL) was added $Pd(PPh_3)_4$ (0.924 g, 0.800 mmol). The mixture was then heated at 90 °C for 18 h, cooled to rt, poured into hydrochloric acid (1 M, 200 mL), filtered, and washed with water and methanol to give **6b** (1.58 g, 83%) as a yellow solid. Mp 287.4 °C. ^{1}H NMR (400 MHz) δ 2.56 (s, 6H), 7.36−7.41 (m, 2H), 7.46−7.52 (m, 4H), 7.61 (s, 2H), 7.63 (s, 2H), 7.66 (dd, J = 1.6, 8.0 Hz, 2H), 7.68−7.72 (m, 4H), 7.91 (d, J = 8.0 Hz, 2H), 7.91 (s, 2H), 8.10 (t, J = 0.8 Hz, 2H). ^{13}C NMR (100 MHz, 1,1,2,2-tetrachloroethane-d_2 at 120 °C) δ 17.0, 120.5, 124.1, 124.3, 124.7, 125.2, 127.5, 129.0, 129.1, 131.4, 133.7, 136.7, 138.2, 139.4, 141.3, 141.6, 141.9. MS(EI) m/z = 636 (M^+). Anal. calcd for $C_{40}H_{28}S_4$: C, 75.43; H, 4.43%. Found C, 75.16; H, 4.50%.

*2,6-Bis(6-hexylbenzo[b]thiophen-2-yl)-3,7-bis(methylthio)-naphthalene (**6c**).* To a degassed solution of **4c** (2.93 g, 8.5 mmol), **5** (1.83g, 3.5 mmol), and K_2CO_3 (1.93 g, 14.0 mmol) in DMF (70 mL) and water (3.5 mL) was added $Pd(PPh_3)_4$ (0.202 g, 0.175 mmol). The mixture was then heated at 90 °C for 23 h, cooled to rt, poured into hydrochloric acid (1 M, 200 mL), filtered, and washed with water and methanol to give **6c** (1.84 g, 80%) as a yellow solid. Mp 194.0 °C. ^{1}H NMR (400 MHz) δ 0.90 (t, J = 7.2 Hz, 6H), 1.28−1.42 (m, 12H), 1.64−1.73 (m, 4H), 2.52 (s, 6H), 2.75 (t, J = 7.8 Hz, 4H), 7.23 (dd, J = 1.2, 8.0 Hz, 2H), 7.54 (s, 2H), 7.56 (s, 2H), 7.68 (s, 2H), 7.73 (d, J = 8.4 Hz, 2H), 7.86 (s, 2H); ^{13}C NMR (100 MHz) δ 14.3, 16.2, 22.8, 29.1, 31.9, 36.2, 121.4, 123.0, 124.6, 125.7, 128.9, 130.8, 132.8, 136.3, 138.0, 139.8, 140.7; MS (EI) m/z = 652 (M^+); Anal. Calcd for $C_{40}H_{44}S_4$: C, 73.57; H, 6.79%. Found C, 73.20; H, 6.79%.

*2,6-Bis(benzo[b]thiophen-2-yl)-3,7-bis(methylsulfinyl)-naphthalene (**2a**).* To a solution of **6a** (2.73 g, 5.63 mmol) in dichloromethane (200 mL) was added *m*-chloroperoxybenzoic acid (1.95 g, 11.3 mmol) at 0 °C. After stirring for 13 h at rt, the mixture was poured into aqueous K_2CO_3 solution (1 M, 200 mL), extracted with dichloromethane. The combined extracts were washed with aqueous K_2CO_3 solution (1 M, 100 mL), dried over $MgSO_4$, and evaporated to give **2a** (2.90 g, quant) as a yellow solid. Mp 294.4 °C. MS (EI) m/z = 516 (M^+). ^{1}H NMR (400 MHz) δ 2.55, 2.56 (s, 6H), 7.40−7.48 (m, 4H), 7.58 (d, J = 1.6 Hz, 2H), 7.85−7.93 (m, 4H), 8.19 (d, J = 2.8 Hz, 2H), 8.70 (d, J = 1.6 Hz, 2H). ^{13}C NMR (100 MHz) δ 42.0, 122.4, 124.4, 124.9, 125.2, 125.5, 130.2, 131.2, 133.3, 138.2, 138.3, 140.0, 140.4, 145.2. HRMS (APCI), m/z calcd for $C_{28}H_{20}O_2S_4$ $[M]^+$: 516.0346. Found: 516.0341. Note that the methylsulfinyl moiety affords two singlets (δ 2.55 and 2.56) in the ^{1}H NMR spectrum owing to the existence of diastereomers.

*2,6-Bis(6-phenylbenzo[b]thiophen-2-yl)-3,7-bis(methylsulfinyl)-naphthalene (**2b**).* To a solution of **6b** (0.318 g, 0.5 mmol) in dichloromethane (150 mL) was added *m*-chloroperoxybenzoic acid (0.173 g, 1.0 mmol) at 0 °C. After stirring for 13 h at rt, the mixture was poured into aqueous K_2CO_3 solution (1 M, 20 mL), extracted with dichloromethane (50 mL × 2). The combined extracts were washed with aqueous K_2CO_3 solution (1 M, 40 mL), dried ($MgSO_4$), and evaporated to give **2b** (0.315 g, 94%) as a pale yellow solid. Mp 273.1 °C. ^{1}H NMR (400 MHz) δ 2.57, 2.59 (s, 6H), 7.38−7.43 (m, 2H), 7.47−7.54 (m, 4H), 7.61 (s, 2H), 7.68−7.72 (m, 4H), 7.70 (d, J = 8.0 Hz, 2H), 7.94 (d, J = 8.0 Hz, 2H), 8.12 (s, 2H), 8.23 (s, 2H), 8.73 (s, 2H). ^{13}C NMR (100 MHz) δ 42.1, 120.6, 124.6, 125.0, 127.5, 127.7, 129.1, 130.2, 131.2, 133.4, 138.5, 138.9, 139.1, 140.7, 141.2, 145.2. MS (EI) m/z = 668 (M^+). HRMS (APCI) calcd for $C_{40}H_{29}O_2S_4$ $[MH]^+$: 669.1050. Found: 669.1049. Note that the methylsulfinyl moiety affords two singlets (δ 2.57 and 2.59) in the ^{1}H NMR spectrum owing to the existence of diastereomers.

*2,6-Bis(6-hexylbenzo[b]thiophen-2-yl)-3,7-di(methylsulfinyl)-naphthalene (**2c**).* To a solution of **6c** (0.196 g, 0.3 mmol) in dichloromethane (40 mL) was added *m*-chloroperoxybenzoic acid (0.104 g, 0.6 mmol) at 0 °C. After stirring for 13 h at rt, the mixture was poured into an aqueous K_2CO_3 solution (20 mL), extracted with dichloromethane (50 mL × 2). The combined extracts were washed with aqueous K_2CO_3 solution (1 M, 40 mL), dried over $MgSO_4$, and evaporated to give **2c** (0.199 g, 97%) as a pale yellow solid. Mp 219.4 °C. ^{1}H NMR (400 MHz) δ 0.90 (t, J = 6.8 Hz, 6H), 1.26−1.45 (m, 12H), 1.64−1.77 (m, 4H), 2.53, 2.55 (s, 6H), 2.76 (t, J = 7.6 Hz, 4H), 7.28 (d, J = 7.6 Hz, 2H), 7.52 (s, 2H), 7.69 (s, 2H), 7.77 (d, J = 8.4 Hz, 2H), 8.16 (d, J = 4.0 Hz, 2H), 8.68 (d, J = 4.0 Hz, 2H). ^{13}C NMR (100 MHz) δ 14.3, 22.7, 29.1, 31.7, 31.8, 36.2, 42.1, 121.5, 124.1, 124.7, 124.8, 126.4, 130.2, 131.1, 133.3, 137.1, 138.1, 140.8, 145.1. HRMS (APCI) m/z calcd for $C_{40}H_{44}NaO_2S_4$ $[MNa]^+$: 707.2122. Found: 707.2128. Note that the methylsulfinyl moiety affords two singlets (δ 2.53 and 2.55) in the ^{1}H NMR spectrum owing to the existence of diastereomers.

Bis[1]benzothieno[2,3-d;2′,3′-d′]naphtho[2,3-b;6,7-b′]-dithiophene (BBTNDT). Under nitrogen atmosphere, **2a** (2.82 g, 5.45 mmol) and P_2O_5 (0.387 g, 2.72 mmol) was added to trifluoromethanesulfonic acid (30 mL). The reaction mixture was stirred at rt for 72 h, poured into ice−water (50 mL), and filtered. The filtrate was washed with water and added to pyridine (50 mL), and the resulting mixture was refluxed for 24 h, poured into methanol, and filtrated. The crude product was extracted with hot *N*-methylpyrrolidone (NMP, 150 mL, 180 °C) in 1 h. After cooling the solution to rt, resulting precipitate was collected by filtration, washed with methanol, and dried. Repeated vacuum sublimation with temperature gradient gave analytical BBTNDT (0.75 g, 33%) as a yellow solid. Mp > 300 °C. MS (EI) m/z = 452 (M^+). Anal. calcd for $C_{26}H_{12}S_4$: C, 68.99; H, 2.67%. Found C, 68.87; H, 2.62%.

2,10-Diphenylbis[1]benzothieno[2,3-d;2′,3′-d′]naphtho[2,3-b;6,7-b′]dithiophene (DPh-BBTNDT). Under nitrogen atmosphere, **2b** (0.308 g, 0.46 mmol) and P_2O_5 (0.033 g, 0.23 mmol) was added to trifluoromethanesulfonic acid (10 mL). The reaction mixture was stirred at rt for 70 h, poured into ice−water (50 mL), and filtered. The filtrate was washed with water and added to pyridine (50 mL), refluxed for 22 h, poured into methanol, and filtered. The crude product was dissolved into NMP (50 mL) at 180 °C in 1 h. After cooling the solution to rt, resulting precipitate was collected by filtration, washed with methanol, and dried. Repeated vacuum sublimation with temperature gradient gave analytical DPh-BBTNDT (0.090 g, 32%) as an orange solid. Mp > 300 °C. Anal. calcd for $C_{38}H_{20}S_4$: C, 75.46; H, 3.33%. Found C, 75.47; H, 3.43%.

2,10-Dihexylbis[1]benzothieno[2,3-d;2′,3′-d′]naphtho[2,3-b;6,7-b′]dithiophene (C6-BBTNDT). Under nitrogen atmosphere, **2c** (0.199 g, 5.45 mmol) and P_2O_5 (0.021 g, 0.145 mmol) was added to trifluoromethanesulfonic acid (5 mL). The reaction mixture was stirred at rt for 68 h, poured into ice−water (50 mL), and filtered. The filtrate was washed with water and dissolved into pyridine (15 mL),

DOI: 10.1021/acs.chemmater.5b01608
Chem. Mater. 2015, 27, 5049−5057

refluxed for 44 h, poured into methanol, and filtrated. The crude product was dissolved into NMP (12 mL) at 180 °C in 1 h. After cooling the solution to rt, resulting precipitate was collected by filtration, washed with methanol, and dried. Repeated vacuum sublimation with temperature gradient gave analytical C6-BBTNDT (0.040 g, 22%) as an orange solid. Mp > 300 °C. ^{1}H NMR (400 MHz, 1,1,2,2-tetrachloroethane-d_2 at 120 °C) δ 0.97 (broad triplet, 6H), 1.35−1.55 (m, 12H), 1.75−1.85 (m, 4H), 2.84 (t, J = 8.4 Hz, 4H), 7.36 (d, J = 7.8 Hz, 2H), 7.80 (s, 2H), 7.82 (d, J = 7.8 Hz, 2H), 8.40 (s, 2H), 8.55 (s, 2H). Anal. calcd for $C_{38}H_{36}S_4$: C, 73.50; H, 5.84%. Found: C, 73.40; H, 5.85%. HRMS (APCI) m/z calcd for $C_{38}H_{36}S_4$ $[M]^+$: 620.1700. Found: 620.1712.

Device Fabrication and Characterization. Field-effect transistors with a "bottom-gate, top-contact" configuration were fabricated in on a heavily doped n^+-Si (100) wafer with a 200 nm thermally grown SiO_2 (C_i = 17.3 nF cm^{-2}). The substrate surfaces were treated with HMDS, OTS, or ODTS as reported previously.[16] A thin film of the organic semiconductors as the active layer was vacuum deposited on the Si/SiO_2 substrates maintained at various substrate temperatures (T_{sub}) at a deposition rate of 1.0 Å s^{-1} under a pressure of ∼10^{-3} Pa. On top of the organic thin film, gold films (80 nm) as drain and source electrodes were deposited through a shadow mask. For a typical device, the drain-source channel length (L) and width (W) are 40 μm and 1.5 mm, respectively. Characteristics of the OFET devices were measured at rt under ambient conditions with a Keithley 4200 semiconducting parameter analyzer. Field-effect mobility (μ_{FET}) was calculated in the saturation regime ($V_d = V_g = -60$ V) of the I_d using the following equation

$$I_d = C_i \mu_{FET} (W/2L)(V_g - V_{th})^2$$

where C_i is the capacitance of the SiO_2 insulator, and V_g and V_{th} are the gate and threshold voltages, respectively. Current on/off ratio (I_{on}/I_{off}) was determined from the I_d at V_g = 0 V (I_{off}) and V_g = −60 V (I_{on}). The μ_{FET} data reported are typical values from more than 10 different devices.

Thermal Stability Tests of the Devices. Test devices were fabricated as mentioned above under identical conditions (T_{sub} = 200 °C for DPh-BBTNDT and C6-BBTNDT, T_{sub} = 100 °C for BBTNDT, deposition rate = 1 Å s^{-1}). The fresh device characteristics were evaluated as mentioned above and defined as the pristine. Then, the same devices were thermally annealed at 100 °C for 30 min in air, cooled to rt, and the device characteristics were measured. The same procedure was performed at 150, 200, 250, and 300 °C, respectively, to evaluate the thermal annealing effects.

X-ray Crystallographic Analyses. Single crystals of DPh-BBTNDT suitable to single crystal X-ray structural analysis were obtained by physical vapor transport.[47] The X-ray crystal structure analysis of DPh-BBTNDT was made by a synchrotron radiation facility in SPring-8 (BL02B1). The structure was solved by the direct methods. Non-hydrogen atoms were refined anisotropically, and hydrogen atoms were included in the calculations but not refined. All calculations were performed using the crystallographic software package SHELXL-2014.[50]

Crystallographic Data for DPh-BBTNDT. $C_{38}H_{20}S_4$ (604.78), yellow plate, 0.08 × 0.05 × 0.003 mm^3, *monoclinic*, space group, $P2_1/a$ (#14), a = 6.1280(15), b = 7.5805(19), c = 28.009(7) Å, β = 94.509(7)°, V = 1297.1(6) Å^3, Z = 2, R = 0.0803 for 2951 observed reflections ($I > 2\sigma(I)$) and 190 variable parameters, w$R2$ = 0.1875 for all data.

■ ASSOCIATED CONTENT

Supporting Information

NMR spectra, CIF for DPh-BBTNDT, and simulated molecular structures optimized by the DFT calculations. The Supporting Information is available free of charge on the ACS Publications website at DOI: 10.1021/acs.chemmater.5b01608.

■ AUTHOR INFORMATION

Corresponding Author

*E-mail: takimiya@riken.jp.

Author Contributions

All authors have given approval to the final version of the manuscript.

Notes

The authors declare no competing financial interest.

■ ACKNOWLEDGMENTS

This work was financially supported by Grants-in-Aid for Scientific Research (Nos. 23245041 and 15H02196) from MEXT, Japan. HRMSs were carried out at the Materials Characterization Support Unit in RIKEN Advanced Technology Support Division. The DFT calculations using the ADF program were performed by using the RIKEN Integrated Cluster of Clusters (RICC). The synchrotron radiation experiments were performed at the BL02B1 of SPring-8 with the approval of the Japan Synchrotron Radiation Research Institute (JASRI) (Proposal No. 2014B1514).

■ REFERENCES

(1) *Organic Electronics, Manufacturing and Applications*; Klauk, H., Ed.; Wiley-VCH: Weinheim, 2006.

(2) *Organic Field-Effect Transistors*; Bao, Z., Locklin, J., Eds.; CRC Press: Boca Raton, 2007.

(3) *Organic Electronics II: More Materials and Applications*; Klauk, H., Ed; Wiley-VCH: Weinheim, 2012.

(4) Dimitrakopoulos, C. D.; Malenfant, P. R. L. Organic Thin Film Transistors for Large Area Electronics. *Adv. Mater.* **2002**, *14*, 99−117.

(5) Anthony, J. E. Functionalized Acenes and Heteroacenes for Organic Electronics. *Chem. Rev.* **2006**, *106*, 5028−5048.

(6) Murphy, A. R.; Frechet, J. M. J. Organic Semiconducting Oligomers for Use in Thin Film Transistors. *Chem. Rev.* **2007**, *107*, 1066−1096.

(7) Klauk, H. Organic thin-film transistors. *Chem. Soc. Rev.* **2010**, *39*, 2643−2666.

(8) Gundlach, D. J.; Lin, Y. Y.; Jackson, T. N.; Nelson, S. F.; Schlom, D. G. Pentacene organic thin-film transistors-molecular ordering and mobility. *IEEE Electron Device Lett.* **1997**, *18*, 87−89.

(9) Lin, Y. Y.; Gundlach, D. J.; Nelson, S. F.; Jackson, T. N. Stacked pentacene layer organic thin-film transistors with improved characteristics. *IEEE Electron Device Lett.* **1997**, *18*, 606−608.

(10) Klauk, H.; Halik, M.; Zschieschang, U.; Eder, F.; Schmid, G.; Dehm, C. Pentacene organic transistors and ring oscillators on glass and on flexible polymeric substrates. *Appl. Phys. Lett.* **2003**, *82*, 4175−4177.

(11) Kelley, T. W.; Boardman, L. D.; Dunbar, T. D.; Muyres, D. V.; Pellerite, M. J.; Smith, T. P. High-Performance OTFTs Using Surface-Modified Alumina Dielectrics. *J. Phys. Chem. B* **2003**, *107*, 5877−5881.

(12) Kitamura, M.; Arakawa, Y. Pentacene-based organic field-effect transistors. *J. Phys.: Condens. Matter.* **2008**, *20*, 184011.

(13) Sirringhaus, H. Device Physics of Solution-Processed Organic Field-Effect Transistors. *Adv. Mater.* **2005**, *17*, 2411−2425.

(14) Allard, S.; Forster, M.; Souharce, B.; Thiem, H.; Scherf, U. Organic Semiconductors for Solution-Processable Field-Effect Transistors (OFETs). *Angew. Chem., Int. Ed.* **2008**, *47*, 4070−4098.

(15) Klauk, H.; Zschieschang, U.; Pflaum, J.; Halik, M. Ultralow-power organic complementary circuits. *Nature* **2007**, *445*, 745−748.

(16) Takimiya, K.; Ebata, H.; Sakamoto, K.; Izawa, T.; Otsubo, T.; Kunugi, Y. 2,7-Diphenyl[1]benzothieno[3,2-*b*]benzothiophene, A New Organic Semiconductor for Air-Stable Organic Field-Effect Transistors with Mobilities up to 2.0 cm^2 V^{-1} s^{-1}. *J. Am. Chem. Soc.* **2006**, *128*, 12604−12605.

(17) Ebata, H.; Izawa, T.; Miyazaki, E.; Takimiya, K.; Ikeda, M.; Kuwabara, H.; Yui, T. Highly Soluble [1]Benzothieno[3,2-*b*]-

DOI: 10.1021/acs.chemmater.5b01608
Chem. Mater. 2015, 27, 5049−5057

benzothiophene (BTBT) Derivatives for High-Performance, Solution-Processed Organic Field-Effect Transistors. *J. Am. Chem. Soc.* **2007**, *129*, 15732−15733.
(18) Izawa, T.; Miyazaki, E.; Takimiya, K. Solution-Processible Organic Semiconductors Based on Selenophene-Containing Heteroarenes, 2,7-Dialkyl[1]benzoselenopheno[3,2-*b*][1]benzoselenophenes (C_n-BSBSs): Syntheses, Properties, Molecular Arrangements, and Field-Effect Transistor Characteristics. *Chem. Mater.* **2009**, *21*, 903−912.
(19) Yamamoto, T.; Takimiya, K. Facile Synthesis of Highly π-Extended Heteroarenes, Dinaphtho[2,3-*b*:2′,3′-*f*]chalcogenopheno[3,2-*b*]chalcogenophenes, and Their Application to Field-Effect Transistors. *J. Am. Chem. Soc.* **2007**, *129*, 2224−2225.
(20) Yamamoto, T.; Shinamura, S.; Miyazaki, E.; Takimiya, K. Three Structural Isomers of Dinaphthothieno[3,2-*b*]thiophenes: Elucidation of Physicochemical Properties, Crystal Structures, and Field-Effect Transistor Characteristics. *Bull. Chem. Soc. Jpn.* **2010**, *83*, 120−130.
(21) Zschieschang, U.; Ante, F.; Yamamoto, T.; Takimiya, K.; Kuwabara, H.; Ikeda, M.; Sekitani, T.; Someya, T.; Kern, K.; Klauk, H. Flexible Low-Voltage Organic Transistors and Circuits Based on a High-Mobility Organic Semiconductor with Good Air Stability. *Adv. Mater.* **2010**, *22*, 982−985.
(22) Zschieschang, U.; Ante, F.; Kälblein, D.; Yamamoto, T.; Takimiya, K.; Kuwabara, H.; Ikeda, M.; Sekitani, T.; Someya, T.; Nimoth, J. B.; Klauk, H. Dinaphtho[2,3-*b*:2′,3′-*f*]thieno[3,2-*b*]-thiophene (DNTT) thin-film transistors with improved performance and stability. *Org. Electron.* **2011**, *12*, 1370−1375.
(23) Takimiya, K.; Osaka, I.; Mori, T.; Nakano, M. Organic Semiconductors Based on [1]Benzothieno[3,2-*b*][1]benzothiophene Substructure. *Acc. Chem. Res.* **2014**, *47*, 1493−1502.
(24) Zschieschang, U.; Yamamoto, T.; Takimiya, K.; Kuwabara, H.; Ikeda, M.; Sekitani, T.; Someya, T.; Klauk, H. Organic Electronics on Banknotes. *Adv. Mater.* **2011**, *23*, 654−658.
(25) Kuribara, K.; Wang, H.; Uchiyama, N.; Fukuda, K.; Yokota, T.; Zschieschang, U.; Jaye, C.; Fischer, D.; Klauk, H.; Yamamoto, T.; Takimiya, K.; Ikeda, M.; Kuwabara, H.; Sekitani, T.; Loo, Y.-L.; Someya, T. Organic transistors with high thermal stability for medical applications. *Nat. Commun.* **2012**, *3*, 723.
(26) Kaltenbrunner, M.; Sekitani, T.; Reeder, J.; Yokota, T.; Kuribara, K.; Tokuhara, T.; Drack, M.; Schwodiauer, R.; Graz, I.; Bauer-Gogonea, S.; Bauer, S.; Someya, T. An ultra-lightweight design for imperceptible plastic electronics. *Nature* **2013**, *499*, 458−463.
(27) Goldmann, C.; Haas, S.; Krellner, C.; Pernstich, K. P.; Gundlach, D. J.; Batlogg, B. Hole mobility in organic single crystals measured by a "flip-crystal" field-effect technique. *J. Appl. Phys.* **2004**, *96*, 2080−2086.
(28) Watanabe, M.; Chang, Y. J.; Liu, S.-W.; Chao, T.-H.; Goto, K.; Islam, M. M.; Yuan, C.-H.; Tao, Y.-T.; Shinmyozu, T.; Chow, T. J. The synthesis, crystal structure and charge-transport properties of hexacene. *Nat. Chem.* **2012**, *4*, 574−578.
(29) Yu, H.; Li, W.; Tian, H.; Wang, H.; Yan, D.; Zhang, J.; Geng, Y.; Wang, F. Benzothienobenzothiophene-Based Conjugated Oligomers as Semiconductors for Stable Organic Thin-Film Transistors. *ACS Appl. Mater. Interfaces* **2014**, *6*, 5255−5262.
(30) Niebel, C.; Kim, Y.; Ruzié, C.; Karpinska, J.; Chattopadhyay, B.; Schweicher, G.; Richard, A.; Lemaur, V.; Olivier, Y.; Cornil, J.; Kennedy, A. R.; Diao, Y.; Lee, W. Y.; Mannsfeld, S.; Bao, Z.; Geerts, Y. H. Thienoacene dimers based on the thieno[3,2-*b*]thiophene moiety: synthesis, characterization, and electronic properties. *J. Mater. Chem. C* **2015**, *3*, 674−685.
(31) Niimi, K.; Shinamura, S.; Osaka, I.; Miyazaki, E.; Takimiya, K. Dianthra[2,3-b:2′,3′-*f*]thieno[3,2-*b*]thiophene (DATT): Synthesis, Characterization, and FET Characteristics of New π-Extended Heteroarene with Eight Fused Aromatic Rings. *J. Am. Chem. Soc.* **2011**, *133*, 8732−8739.
(32) Mori, T.; Nishimura, T.; Yamamoto, T.; Doi, I.; Miyazaki, E.; Osaka, I.; Takimiya, K. Consecutive Thiophene-Annulation Approach to π-Extended Thienoacene-Based Organic Semiconductors with [1]Benzothieno[3,2-*b*][1]benzothiophene (BTBT) Substructure. *J. Am. Chem. Soc.* **2013**, *135*, 13900−13913.
(33) Kang, M. J.; Doi, I.; Mori, H.; Miyazaki, E.; Takimiya, K.; Ikeda, M.; Kuwabara, H. Alkylated Dinaphtho[2,3-*b*:2′,3′-*f*]Thieno[3,2-*b*]Thiophenes (C_n-DNTTs): Organic Semiconductors for High-Performance Thin-Film Transistors. *Adv. Mater.* **2011**, *23*, 1222−1225.
(34) Kang, M. J.; Miyazaki, E.; Osaka, I.; Takimiya, K.; Nakao, A. Diphenyl Derivatives of Dinaphtho[2,3-*b*:2′,3′-*f*]thieno[3,2-*b*]-thiophene: Organic Semiconductors for Thermally Stable Thin-Film Transistors. *ACS Appl. Mater. Interfaces* **2013**, *5*, 2331−2336.
(35) Yokota, T.; Kuribara, K.; Tokuhara, T.; Zschieschang, U.; Klauk, H.; Takimiya, K.; Sadamitsu, Y.; Hamada, M.; Sekitani, T.; Someya, T. Flexible Low-Voltage Organic Transistors with High Thermal Stability at 250 °C. *Adv. Mater.* **2013**, *25*, 3639−3644.
(36) Sirringhaus, H.; Friend, R. H.; Wang, C.; Leuninger, J.; Müllen, K. Dibenzothienobisbenzothiophene-a novel fused-ring oligomer with high field-effect mobility. *J. Mater. Chem.* **1999**, *9*, 2095−2101.
(37) Gao, P.; Beckmann, D.; Tsao, H. N.; Feng, X.; Enkelmann, V.; Baumgarten, M.; Pisula, W.; Müllen, K. Dithieno[2,3-*d*:2′,3′-*d*′]benzo-[1,2-*b*:4,5-*b*′]dithiophene (DTBDT) as Semiconductor for High-Performance, Solution-Processed Organic Field-Effect Transistors. *Adv. Mater.* **2009**, *21*, 213−216.
(38) Huang, J.; Luo, H.; Wang, L.; Guo, Y.; Zhang, W.; Chen, H.; Zhu, M.; Liu, Y.; Yu, G. Dibenzoannelated Tetrathienoacene: Synthesis, Characterization, and Applications in Organic Field-Effect Transistors. *Org. Lett.* **2012**, *14*, 3300−3303.
(39) Liu, X.; Wang, Y.; Gao, J.; Jiang, L.; Qi, X.; Hao, W.; Zou, S.; Zhang, H.; Li, H.; Hu, W. Easily solution-processed, high-performance microribbon transistors based on a 2D condensed benzothiophene derivative. *Chem. Commun.* **2014**, *50*, 442−444.
(40) Niculescu-Duvaz, D.; Niculescu-Duvaz, I.; Suijkerbuijk, B. M. J. M.; Ménard, D.; Zambon, A.; Davies, L.; Pons, J.-F.; Whittaker, S.; Marais, R.; Springer, C. J. Potent BRAF kinase inhibitors based on 2,4,5-trisubstituted imidazole with naphthyl and benzothiophene 4-substituents. *Bioorg. Med. Chem.* **2013**, *21*, 1284−1304.
(41) Takimiya, K.; Yamamoto, T.; Ebata, H.; Izawa, T. Design strategy for air-stable organic semiconductors applicable to high-performance field-effect transistors. *Sci. Technol. Adv. Mater.* **2007**, *8*, 273−276.
(42) Anthopoulos, T. D.; Anyfantis, G. C.; Papavassiliou, G. C.; de Leeuw, D. M. Air-stable ambipolar organic transistors. *Appl. Phys. Lett.* **2007**, *90*, 122105.
(43) Takimiya, K.; Osaka, I.; Nakano, M. π-Building Blocks for Organic Electronics: Revaluation of "Inductive" and "Resonance" Effects of π-Electron Deficient Units. *Chem. Mater.* **2014**, *26*, 587−593.
(44) Dong, H.; Fu, X.; Liu, J.; Wang, Z.; Hu, W. 25th Anniversary Article: Key Points for High-Mobility Organic Field-Effect Transistors. *Adv. Mater.* **2013**, *25*, 6158−6183.
(45) Schweicher, G.; Olivier, Y.; Lemaur, V.; Geerts, Y. H. What Currently Limits Charge Carrier Mobility in Crystals of Molecular Semiconductors? *Isr. J. Chem.* **2014**, *54*, 595−6183.
(46) Park, J.-I.; Chung, J. W.; Kim, J.-Y.; Lee, J.; Jung, J. Y.; Koo, B.; Lee, B.-L.; Lee, S. W.; Jin, Y. W.; Lee, S. Y. Dibenzothiopheno[6,5-*b*:6′,5′-*f*]thieno[3,2-*b*]thiophene (DBTTT): High-Performance Small-Molecule Organic Semiconductor for Field-Effect Transistors. *J. Am. Chem. Soc.* **2015**, DOI: 10.1021/jacs.5b01108.
(47) Laudise, R. A.; Kloc, C.; Simpkins, P. G.; Siegrist, T. J. Physical vapor growth of organic semiconductors. *Cryst. Growth* **1998**, *187*, 449−454.
(48) ADF: powerful DFT code for modeling molecules. http://www.scm.com/ADF/ (accessed April 3, 2015).
(49) Takimiya, K.; Shinamura, S.; Osaka, I.; Miyazaki, E. Thienoacene-Based Organic Semiconductors. *Adv. Mater.* **2011**, *23*, 4347−4370.
(50) Sheldrick, G. Crystal structure refinement with SHELXL. *Acta Crystallogr., Sect. C: Struct. Chem.* **2015**, *71*, 3−8.

DOI: 10.1021/acs.chemmater.5b01608
Chem. Mater. 2015, 27, 5049−5057